

Article

A New Constitutive Relation for Homogeneous Isotropic Materials by FEM Model of the Brazilian Splitting Test

Salvatore Benfratello , Antonino Cirello  and Luigi Palizzolo 

Department of Engineering, University of Palermo, Viale delle Scienze, Building 8, 90128 Palermo, Italy; antonino.cirello@unipa.it (A.C.); luigi.palizzolo@unipa.it (L.P.)

* Correspondence: salvatore.benfratello@unipa.it

Abstract

The paper studies the behavior of homogeneous isotropic materials by performing appropriate numerical analyses and utilizing suitable FEMs to reproduce the Brazilian splitting test. Starting with a theoretical approach and adopting suitable numerical simulations, a new formula that is able to characterize the Young's modulus is presented. To this end, in addition to the analysis of the specimen's response in terms of stresses and strains, the real displacement field resulting from the real kinematical constraints on the specimen is determined. Therefore, the Brazilian test is taken as a reference test and the specimen's behavior is derived by taking advantage of both the theoretical approach and numerical simulations developed in the ANSYS 2021 R1 environment. The latter allows us to define a new mathematical relation representing the missing part of the kinematical field. Furthermore, a new formula which explicitly relates the Young's modulus of the material to the geometrical characteristics of the specimen, to the acting force, and to a measured selected displacement is proposed. Future developments will include adopting the proposed formulas for the identification of other mechanical parameters of the material, e.g., by adopting a full-field contactless approach to displacement measurement and studying the behavior of specimens with different geometrical characteristics.

Keywords: Brazilian splitting test; mechanical parameter identification; kinematical behavior; homogeneous isotropic material; nonuniform stress; FEM; numerical simulations



Academic Editor: Aires Camões

Received: 10 June 2025

Revised: 14 July 2025

Accepted: 31 July 2025

Published: 3 August 2025

Citation: Benfratello, S.; Cirello, A.; Palizzolo, L. A New Constitutive Relation for Homogeneous Isotropic Materials by FEM Model of the Brazilian Splitting Test. *Sci* **2025**, *7*, 110. <https://doi.org/10.3390/sci7030110>

Copyright: © 2025 by the authors. Licensee MDPI, Basel, Switzerland. This article is an open access article distributed under the terms and conditions of the Creative Commons Attribution (CC BY) license (<https://creativecommons.org/licenses/by/4.0/>).

1. Introduction

The indirect tensile test is an experimental test that is largely adopted to determine the tensile strength of brittle materials, both in the geotechnical field (specifically in the field of rock mechanics) and in the structural one (specifically in the field of cementitious materials). The test [1,2] was created and proposed by the Brazilian engineer Fernando Lobo Carneiro at the beginning of the 1940s to determine the tensile strength of concrete cylinders. The latter mechanical problem became necessary to evaluate the possibility of adopting concrete cylinders in place of steel ones for the repositioning of a historical church in Rio de Janeiro. The proposed test achieved resounding success at the international level, and since it was conducted by Lobo Carneiro, scientists began to refer to the indirect tensile test as the Brazilian test. Nowadays, this test is widely adopted in all international standards (see, e.g., [3–6]) and it plays a fundamental role in the evaluation of the mechanical characteristics of specimens obtained by suitable coring in existing structures. Mainly, this test is performed by compressing a cylindrical specimen along two

opposite diametral generatrices. The break of the specimen occurs on the plane containing the loaded generatrices, due to tensile stresses orthogonal to that plane.

The ability of the Brazilian test to create a nonuniform stress field has been adopted in recent papers to identify the mechanical characteristics of anisotropic materials such as shale [7] and fiber-reinforced cementitious materials [8,9], with the latter materials being of particular interest to both construction and extractive industries.

From a theoretical point of view, this problem has been faced by many authors, such as Timoshenko and Goodier [10]. They analyzed the stress field in a circular disk subjected to two opposing concentrated forces applied to the circumference representing the disk contour. These results have been largely adopted in the literature (see, e.g., [11–17]) to provide insights into the mechanical behavior of brittle and quasi-brittle materials. Other authors (see, e.g., [18,19]) proposed using numerical models for the evaluation of the stress field of a specimen under a Brazilian test.

Furthermore, Jemiolo [20] identified the strain and displacement fields in both the assumptions of plane stress state and plane strain state. It is to be remarked that the displacement field obtained has been considered an ideal model without any kinematical constraint related to the real conditions of the specimen. The role of the contact between the plates of the testing machine and the specimen is discussed in many papers available in the literature (see, e.g., [21–26]), but this role is described with regard to its influence on the stress field rather than on the displacement one.

The Brazilian test has been recently (see, e.g., [27–31]) adopted to carry out the experimental identification of some mechanical parameters (Young's modulus and Poisson's coefficient in addition to the tensile strength), starting from the theoretical model obtained in [10], but the proposed approach takes into account only one component of the displacement, since the corresponding field is not completely known.

On the other hand, the identification process of the Brazilian test has improved greatly due to the development of full-field contactless displacement measurement techniques which, based on different approaches, measure the displacement of the points belonging to the cross-section of the specimen under test. It follows that the adoption of these techniques requires knowledge of the real displacement field acting on the specimen.

The real Brazilian test is performed by a testing machine that possesses a fixed platen and a moving one that applies a load or a displacement to the specimen. From a mechanical point of view, the experimental situation is in accordance with the theoretical one. From a kinematical point of view, on the contrary, the experimental situation is very different from the theoretical one usually considered, due to the absence of kinematical constraints. Indeed, the fixed platen imposes a null displacement on the lower generatrix of the specimen which is not present in the theoretical model. In recent decades, the development of ever-increasing computing power has allowed the development of a new field of scientific research related to numerical algorithms capable of modeling real problems for which the theoretical solution is not available and in wider application fields (see, e.g., [32,33]). Within these techniques, the so-called Finite Element Model approach has often played a fundamental role in the development of new theoretical solutions or in the improvement of existing ones.

In recent years, several authors have investigated the splitting (Brazilian) test both numerically and experimentally across various research domains. For instance, Jing et al. [34] experimentally analyzed how the characteristics, particularly those related to fracture mechanisms, change in thermally treated granite specimens, identifying significant correlations between treatment temperature and fracture behavior. Zhang et al. [35] explored the use of different resin types for repairing fractures in granite, aiming to enhance safety in subsurface engineering applications. They developed an improved specimen model that reduces

asymmetries compared to the classical bi-material model. Li et al. [36] and Kim et al. [37] developed numerical models to study the fracture behavior of prismatic specimens subjected to the Brazilian test with supporting fixtures, using image processing techniques and a phase-field fracture model, respectively. Furthermore, Lei et al. [38] proposed a numerical model for shale specimens, building on Rocco's theoretical framework [39], and incorporating void and defect distributions characterized by CT-scan imaging. None of the aforementioned studies calculated the mechanical properties of the materials based on measured displacements, likely due to the focus on heterogeneous materials, where standard theoretical approaches are not easily applicable and assumptions such as symmetry across the loading axis cannot be strictly satisfied.

The present paper aims to define a new constitutive relation for homogeneous isotropic materials by means of a suitable FEM of the Brazilian splitting test. In particular, a kinematical model of the Brazilian test in real conditions is considered, and the obtained numerical results allow us to gather information on the mechanical behavior of the material. The goal is achieved by starting with the actual model available in the literature and integrating it by adopting the results obtained by numerical simulations performed by ANSYS 2021 R1 software. The numerical simulations have been performed by adopting a wide range for both geometrical and mechanical characteristics; these ranges have been identified considering the regulatory indications as well as the materials (concrete and rocks) usually tested. On the grounds of the obtained results, a new formula that is able to relate the displacement field to the Young's modulus is proposed, and this opens up new and interesting perspectives on the development of identification techniques to determine other mechanical characteristics of the material besides the tensile strength.

2. Materials and Methods

In this section, the approach adopted for the determination of the mechanical behavior of the isotropic material using the Brazilian splitting test is presented. The first subsection reports the basis of the Brazilian splitting test, the solution in terms of stresses available in the literature, and the consequent strain and displacement solutions. The second subsection describes the FEM for the simulation of a real Brazilian splitting test.

2.1. Brazilian Test

The splitting test (see Figure 1), also known as the Brazilian splitting test [1,3–5], is an internationally adopted, effective test for determining the indirect tensile behavior (usually the strength) of brittle materials such as rocks and cementitious ones. The test is performed by placing a cylindrical specimen of known geometrical characteristics (diameter D and depth H) between the plates of the testing machine. A uniformly distributed load p_x is applied on the upper generatrix by the upper platen until the sample is broken.

Initially, contact between the platen and the specimen is produced in a unique contact line. Because of the finite elastic moduli of the involved materials, increments in the load application during test execution cause contact to evolve from a line to an area. Although the specimens are straight cylindrical elastic solids, the analytical approach to the problem can be stated in terms of plane elasticity if the contact stresses are uniformly distributed along the longitudinal direction [2]. Hence, a three-dimensional elastic problem is usually converted into a two-dimensional problem, simplifying its mathematical treatment.

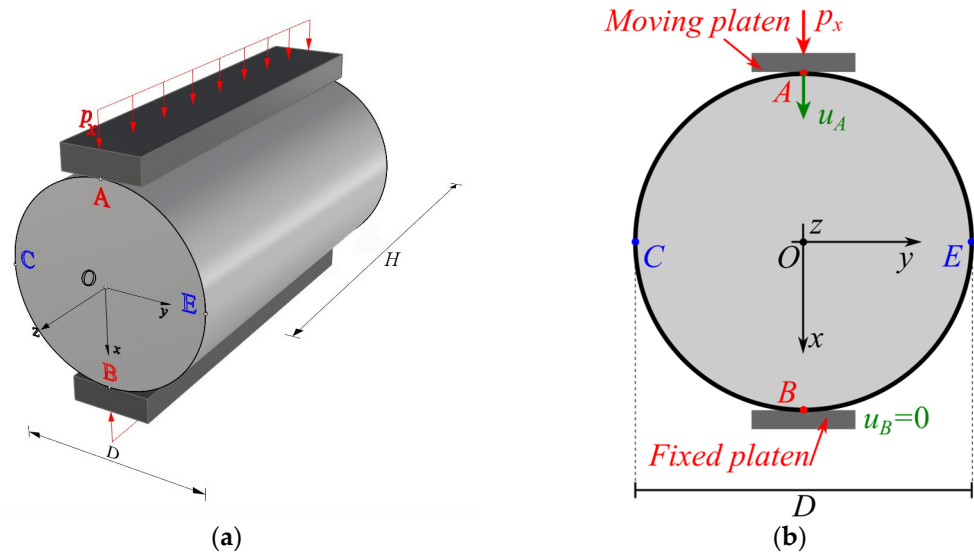


Figure 1. Scheme of the real Brazilian test: (a) 3D sketch; (b) front view.

In the literature [11], the general case of a disk subjected to a couple of opposite concentrated forces P acting along a chord has been studied and the corresponding stress field has been determined under the assumptions of perfectly elastic material. In this framework, the case of the cross-section of a specimen composed of homogeneous linear elastic material subjected to the Brazilian splitting test can be regarded as a special case in which the chord coincides with the vertical diameter (Figure 2) and $P = p_x H$.

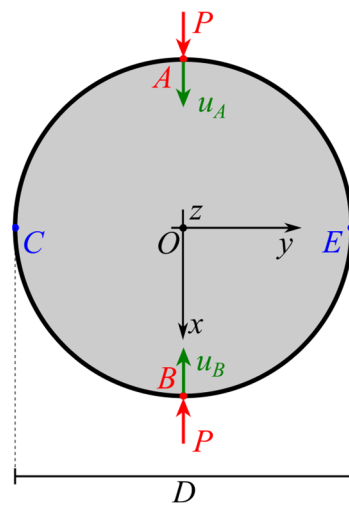


Figure 2. Theoretical model of the Brazilian test $|u_A| = |u_B|$.

The stress, strain, and the corresponding displacement fields arising in the specimen under the test are three-dimensional. However, depending on the ratio between depth and diameter, H/D , the further assumption of plane stress state or plane strain state can be assumed. In the former case, the stress field is given by the following relation [20]:

$$\sigma = \begin{bmatrix} \frac{p_x}{\pi R} - \frac{2p_x \left(\frac{(R-x)^3}{((R-x)^2+y^2)^2} + \frac{(R+x)^3}{((R+x)^2+y^2)^2} \right)}{\pi} & - \frac{2p_x \left(\frac{(R-x)(-R+x)y}{((R-x)^2+y^2)^2} + \frac{(R+x)^2y}{((R+x)^2+y^2)^2} \right)}{\pi} \\ - \frac{2p_x \left(\frac{(R-x)(-R+x)y}{((R-x)^2+y^2)^2} + \frac{(R+x)^2y}{((R+x)^2+y^2)^2} \right)}{\pi} & \frac{p_x}{\pi R} - \frac{2p_x \left(\frac{(R-x)y^2}{((R-x)^2+y^2)^2} + \frac{(R+x)y^2}{((R+x)^2+y^2)^2} \right)}{\pi} \end{bmatrix}, \quad (1)$$

where $R = D/2$. In the case of plane strain state, the following relations hold:

$$\boldsymbol{\varepsilon} = \begin{bmatrix} \varepsilon_x & \gamma_{xy} \\ \gamma_{xy} & \varepsilon_y \end{bmatrix} \tag{2}$$

$$\varepsilon_x = \frac{p_x(1 + \nu) \left\{ \frac{1}{R} - 2 \left[\frac{(R-x)^3}{[(R-x)^2+y^2]^2} + \frac{(R+x)^3}{[(R+x)^2+y^2]^2} \right] + \frac{2\nu[-R^4+(x^2+y^2)^2]}{R[(R-x)^2+y^2][(R+x)^2+y^2](-1-\nu)} \right\}}{E\pi} \tag{3a}$$

$$\varepsilon_y = \frac{p_x(1 + \nu) \left\{ \frac{1}{R} - 2y^2 \left[\frac{R-x}{[(R-x)^2+y^2]^2} + \frac{R+x}{[(R+x)^2+y^2]^2} \right] + \frac{2\nu[-R^4+(x^2+y^2)^2]}{R[(R-x)^2+y^2][(R+x)^2+y^2](-1-\nu)} \right\}}{E\pi} \tag{3b}$$

$$\gamma_{xy} = -\frac{2p_x \left[-\frac{(R-x)^2y}{[(R-x)^2+y^2]^2} + \frac{(R+x)^2y}{[(R+x)^2+y^2]^2} \right] (1 + \nu)}{E\pi} \tag{3c}$$

In [20], the analytical expression for ε_z in the case of plane stress state or that for σ_z in the case of plane strain state can be found.

Considering the mathematical definition of ε_x and ε_y , by integration of Equations (3a) and (3b), and considering Equation (3c), the following equations for the displacements u (along the x -axis) and v (along the y -axis) are obtained:

$$u = \frac{p_x(1+\nu)}{E\pi} \left\{ y^2 \left[\frac{1}{(R-x)^2+y^2} - \frac{1}{(R+x)^2+y^2} \right] + \frac{x-b}{R+(b-2)R\nu} + \frac{[-1+(b-1)\nu] \left[\text{Log}[(R-x)^2+y^2] - \text{Log}[(R+x)^2+y^2] \right]}{-1+(-2+b)\nu} \right\} + C_1(y) \tag{4}$$

$$v = \frac{p_x(1+\nu)}{E\pi} \left\{ y \left[\frac{1}{R} + \frac{R-x}{(R-x)^2+y^2} + \frac{R+x}{(R+x)^2+y^2} - \frac{2\nu}{R-(b-2)R\nu} \right] + \frac{2\nu \left\{ \text{Atan} \left[\frac{R-x}{y} \right] + \text{Atan} \left[\frac{R+x}{y} \right] \right\}}{-1+(b-2)\nu} - \text{Atan} \left[\frac{y}{R-x} \right] - \text{Atan} \left[\frac{y}{R+x} \right] \right\} + C_2(x) \tag{5}$$

In Equations (4) and (5), $C_1(y)$ and $C_2(x)$ are unknown functions to be determined by imposing suitable boundary and symmetry conditions, while the parameter b has been introduced to obtain a unique formula for both the cases of plane stress and plane strain states ($b = 1$ for plane stress state; $b = 2$ for plane strain state) [20]. Both the geometrical symmetry and the mechanical one with respect to the x -axis lead to the consequence that

$$C_2(x) = 0. \tag{6}$$

Furthermore, considering Equations (3c), (4) and (5), the following relation is obtained:

$$C'_1(y) + C'_2(x) = 0 \tag{7}$$

which, because of Equation (6), leads to

$$C'_1(y) = 0 \Rightarrow C_1(y) = cost \tag{8}$$

By comparing Figures 1b and 2, it is evident that the theoretical model shows a double symmetric kinematical condition (either along the x -axis or the y -axis). Consequently, in the theoretical model, the result is as follows:

$$C_1(y) = 0 \quad (9a)$$

$$C_2(x) = 0 \quad (9b)$$

Equation (9a) is valid only in the theoretical model but not in the real condition. It follows that, to characterize the kinematical behavior observed during the Brazilian test, it is necessary to determine (see Equation (4)) $C_1(y) = \bar{u}$, which represents the displacement along the x -axis of the points belonging to the y -axis; this goal is performed by adopting a suitable numerical approach based on the FEM described in the following subsection.

2.2. Numerical FEM

The determination of the constant in Equation (8) cannot be mathematically determined, since all the quantities involved diverge at points A and B. It follows that to characterize the kinematical behavior under the Brazilian splitting test, it is necessary to refer to numerical simulations. The latter have been performed in the ANSYS 2021 R1 Workbench environment, under the hypothesis of linear elastic behavior of the involved materials, by varying the geometrical parameters, the distributed force p_x and the Young's modulus, recording the x -displacement along the y -axis. The Poisson's coefficient has been initially assumed to be $\nu = 0.25$ and its influence has been checked by repeating the analyses, assuming $\nu = 0.10$, as reported at the end of Section 3.

In order to reproduce the real Brazilian test, the numerical model geometry accounts for both the specimen under testing as well as for the presence of two steel plates ($E = 210$ GPa, $\nu = 0.33$; see Figure 3a): one devoted to imposing the kinematical full-restrained constraint on the lower generatrix of the specimen, while the other focuses on applying the distributed load on the upper generatrix of the specimen. The presence of the plates implies the modeling of the contact between the plates and the specimen, which we will describe in this paper. The adopted elements are 10-node isoparametric elements for solid discretization and 8-node 3D solid contact elements for surface-to-surface contact modeling. All the contacts have been modeled as "bonded", as penetration and gaps are not allowed. The large deformation option is set to improve convergence in cases with low stiffness. All analyses have been nonlinear due to contact, but convergence has been gained in a few iterations.

The mesh dimension was selected after suitable preliminary mesh independence investigations that aimed to find the best compromise between results and computational time. This study has been performed by adopting the model with the highest diameter for the cylinder and the lowest Young's modulus value for material stiffness. The final mesh (Figure 3b) leads to a displacement value within 2% of that obtained by doubling the number of elements, presenting about 107,000 elements in total, and all the analyses have the same element distribution. To reduce the computational effort, the geometric numerical model takes into account the symmetry of the real problem. Therefore, the adopted boundary conditions are as follows: (a) symmetry in the vertical diametral faces; (b) fixed support (all displacements are equal to zero) on the lower face of the lower platen (plane B in Figure 3a); (c) surface-distributed force on the upper face of the upper platen (plane A in Figure 3a), and all contact modeled as bounded.

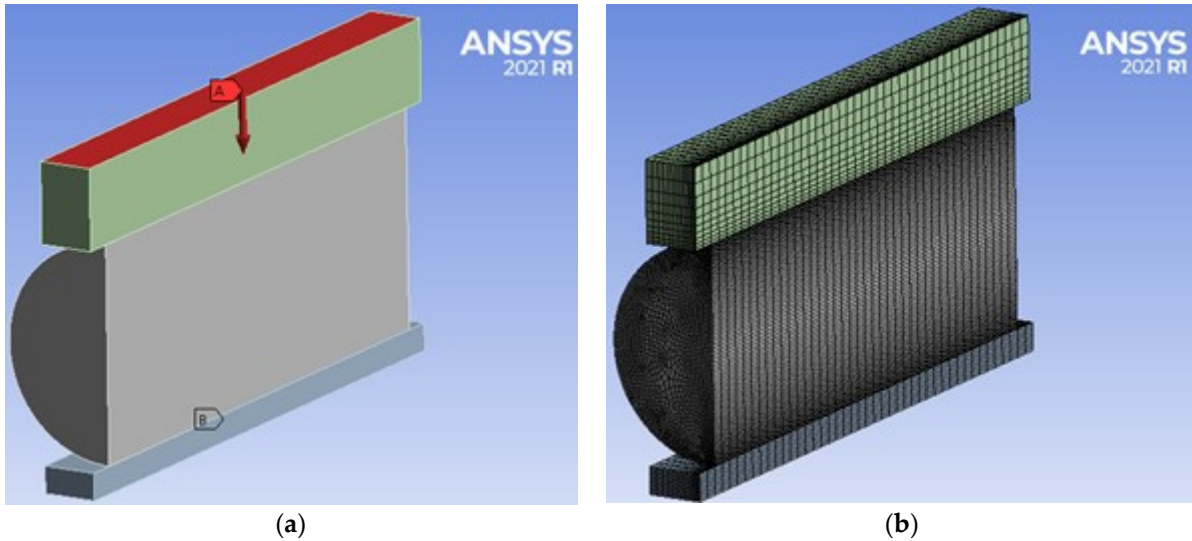


Figure 3. FEM in ANSYS: (a) adopted geometry; (b) adopted mesh.

The steps performed in the numerical analyses are summarized here, while the values of the selected parameters are reported in the following section. For the assigned depth-to-diameter ratio (H/D) and for the selected value of Young’s modulus E , the specimen diameter D was varied within the selected range. For each configuration, the corresponding distributed force applied to the upper plate was calculated based on a prescribed pressure acting at the center of the specimen, as indicated by the relevant international standards. During each simulation, the horizontal displacement u along the specimen’s diameter was recorded and verified to remain effectively constant, with deviations from the mean value remaining below 1%.

3. Results

The analyses reported in this section have been performed with particular focus on the case, as prescribed by international standards, of the ratio between depth and diameter $H/D = 2$, by varying the Young’ modulus in the range $1 \text{ GPa} \leq E \leq 50 \text{ GPa}$ and the diameter in the range $0.02 \text{ m} \leq D \leq 0.1 \text{ m}$ with increments equal to 0.01 m . The main idea is to perform the analyses in such a way that the stress acting at the center of the specimen is considered as constant. The relation between this stress (indicated as $\bar{\sigma}_x$ below) and the total acting force is reported in all international standards, and it is given by

$$\bar{\sigma}_x = \frac{2 P}{\pi D H} \tag{10}$$

The acting force has been determined assuming that $\bar{\sigma}_x$ is in the range of $0.02 \text{ MPa} \leq \bar{\sigma}_x \leq 20 \text{ MPa}$. The assumed values have been selected considering that the Brazilian test is usually performed for rocks and concrete samples.

The results, in terms of displacement \bar{u} vs. the diameter D , are reported in the following Figure 4.

From an examination of Figure 4, it can be stated that the displacement \bar{u} is a linear function of the diameter D and that the slope m of the lines is a function of both the Young’s modulus and $\bar{\sigma}_x$; that is,

$$m = f(\bar{\sigma}_x, E). \tag{11}$$

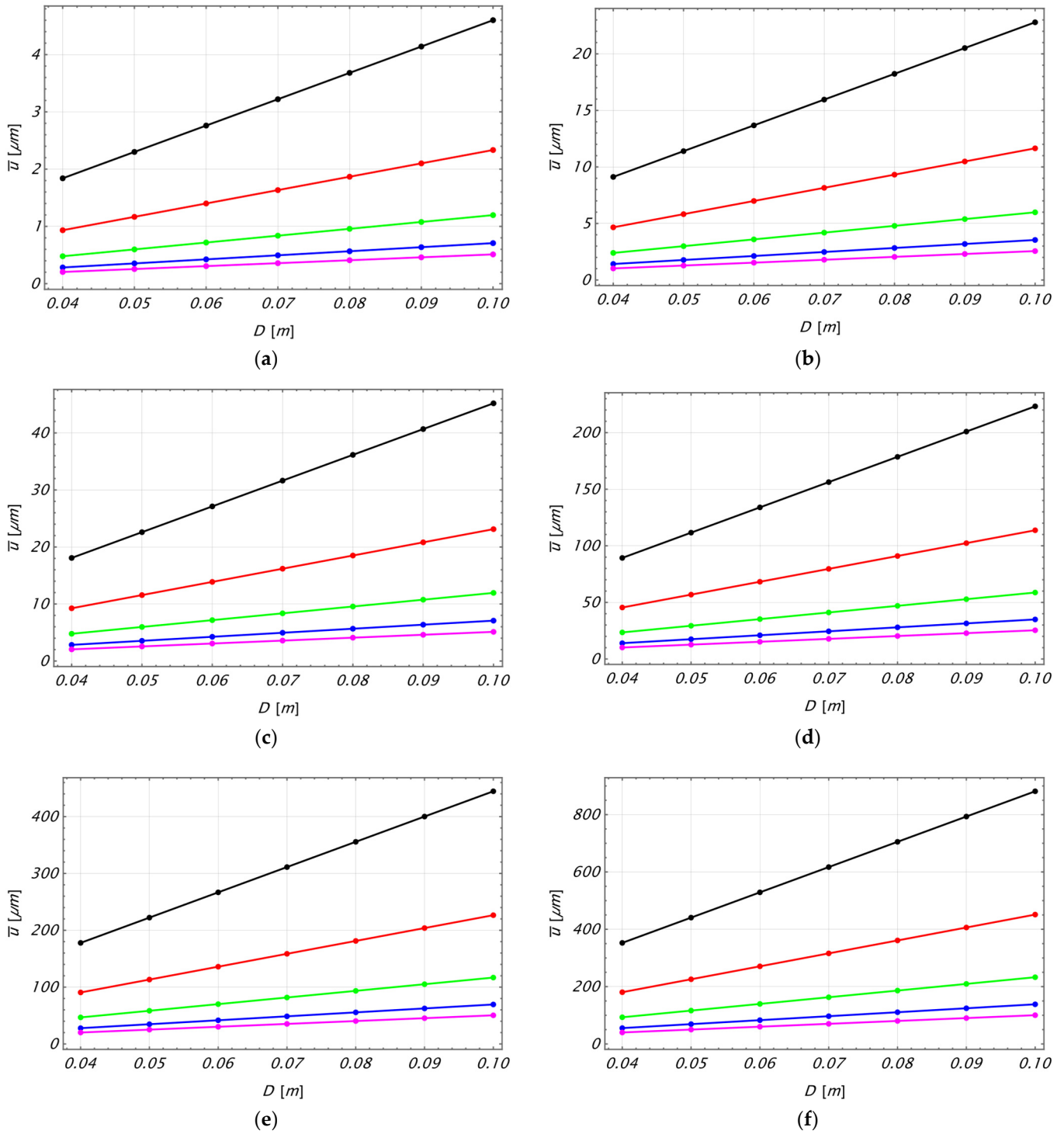


Figure 4. \bar{u} vs. D (black line: $E = 5$ GPa; red line: $E = 10$ GPa, green line: $E = 20$ GPa, blue line: $E = 35$ GPa, fuchsia line: $E = 50$ GPa): (a) $\bar{\sigma}_x=100$ kPa; (b) $\bar{\sigma}_x = 500$ kPa; (c) $\bar{\sigma}_x = 1$ MPa; (d) $\bar{\sigma}_x = 5$ MPa; (e) $\bar{\sigma}_x = 10$ MPa; and (f) $\bar{\sigma}_x = 20$ MPa.

The expression of the function f in Equation (11) must be defined. Since the slope is dimensionless, to check the evolution of the function f , it is straightforward to plot it vs. the ratio $\bar{\sigma}_x/E$, as reported in Figure 5.

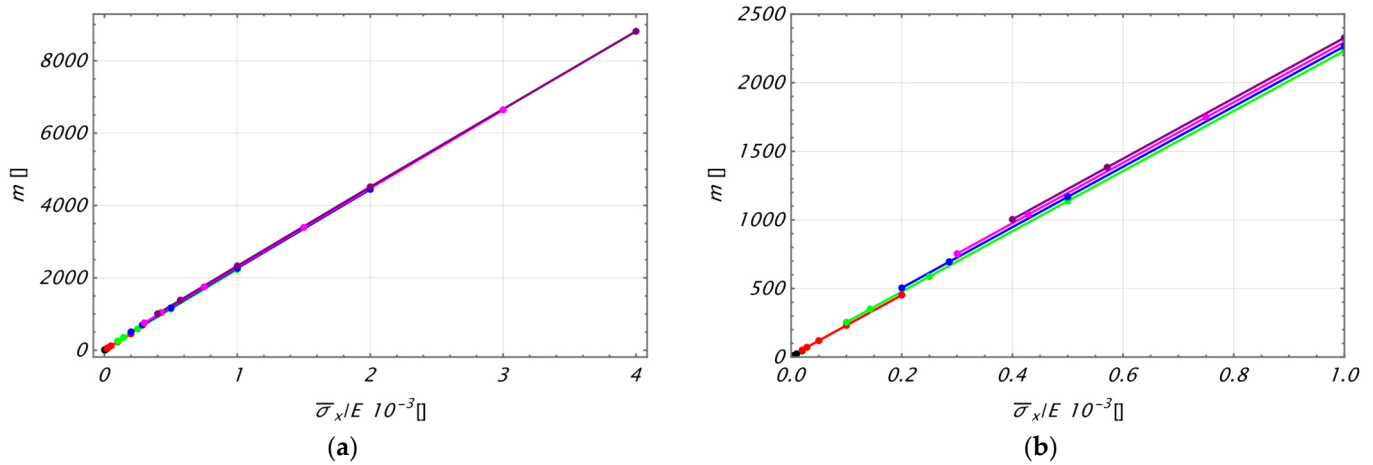


Figure 5. Slope m vs. $\frac{\bar{\sigma}_x}{E}$ (black line: $\bar{\sigma}_x = 0.02$ MPa; red line: $\bar{\sigma}_x = 0.1$ MPa, green line: $\bar{\sigma}_x = 0.5$ MPa, blue line: $\bar{\sigma}_x = 1$ MPa, fuchsia line: $\bar{\sigma}_x = 5$ MPa, purple line: $\bar{\sigma}_x = 20$ MPa): (a) overall view; (b) view of the range $0 \leq \frac{\bar{\sigma}_x}{E} \leq 1$.

An examination of Figure 5 indicates that the slope m is a linear function of the ratio $\bar{\sigma}_x/E$. In Table 1, the values of the slope, determined by the LinearModelFit command available in Mathematica® 14.1 library, are reported.

Table 1. Values of the slopes in Figure 5.

$\bar{\sigma}_x$ [MPa]	Slope's Value m
0.02	2.3158
0.1	2.3158
0.5	2.2993
1.0	2.2813
2.5	2.2617
5.0	2.2513
10.0	2.2242
15.0	2.2336
20.0	2.2248

The examination of Table 1 clearly indicates that the difference between the values of the slope in the first and last case is less than 4%, which can be ascribed to numerical uncertainty. Therefore, the slope's value is herein assumed as a constant and equal to the mean value 2.2695. Assuming this value as the reference one, the error lies in the range $\pm 2\%$. To check the possible influence of the Poisson's coefficient on the results, the numerical simulations have been repeated assuming $\nu = 0.10$, and the obtained results are reported in Table 2.

Table 2. Values of the slopes for $\nu = 0.10$.

$\bar{\sigma}_x$ [MPa]	Slope's Value m
0.02	2.3489
0.1	2.3487
0.5	2.3320
1.0	2.3139
2.5	2.2941
5.0	2.2848
10.0	2.2727
15.0	2.2655
20.0	2.2566

The obtained results are 1% greater than those present in Table 1; therefore, it can be deduced that the value of the slope m is almost independent of the Poisson's coefficient.

The above remarks indicate that the displacement \bar{u} can be obtained by

$$\bar{u} = \alpha \frac{\bar{\sigma}_x}{E} D = \frac{\alpha 2 P}{\pi H E} = \frac{\alpha P}{\pi D E} \quad (12)$$

where $\alpha = 2.2695$. The final Equation (12) has been derived considering that the numerical investigations have been performed for $H/D = 2$, as already stated at the beginning of Section 3.

4. Discussion

The results presented in the foregoing section represent a conclusive step toward understanding the kinematical and mechanical behavior of a specimen of homogeneous isotropic material subjected to the Brazilian test. The obtained results show that the vertical displacement of the horizontal diameter is constant, and it depends linearly on the pressure acting on the horizontal diametral plane of the specimen and inversely on the Young's modulus. Similarly, the acting pressure linearly depends on the acting load and inversely on the diameter; as a consequence, on the whole, the vertical displacement linearly depends on the acting load and inversely on both the diameter and the Young's modulus. This result is physically meaningful, since for a specimen with assigned geometry and material, an increasing load clearly increases the vertical displacement. On the other hand, for an assigned load, the vertical displacement decreases for an increment of the diameter and/or of the Young's modulus. The most notable new result is the evaluation of the constant factor α specializing the relation among the above-described quantities. This result is a novelty, since no other study available in the literature faced the proposed problem leading to an explicit relation as obtained in the foregoing section. Another result is the independence of the considered displacement \bar{u} on the Poisson's coefficient of the material. The latter result is coherent with the theory of isotropic material, in which the Poisson coefficient influences only the kinematical behavior in a transverse direction. The above-reported results can be compared with the corresponding ones arising in a prismatic specimen (square cross-section of side D and depth H , which is a prismatic specimen circumscribed to the cylindrical of the Brazilian splitting test) subjected to a standard compression test. In this case, the theoretical solution leads to the following relation for the vertical displacement of the midplane

$$\bar{u} = \frac{P}{2 H E} = \frac{P}{4 D E} \quad (13)$$

where the latter part of Equation (13) is obtained under the assumption of $H/D = 2$. The comparison between Equations (12) and (13) leads to the remark that, under the same total load P , the displacement \bar{u} is greater in the case of Brazilian splitting test. This result must be ascribed to the difference in the geometry of the two specimens, which leads to different stress and strain fields with the described consequence on the displacement \bar{u} .

5. Conclusions

In this study, the behavior of cylindrical specimens composed of homogeneous and isotropic material subjected to the Brazilian splitting test is investigated through the development of appropriate finite element models implemented within the ANSYS environment. Numerical simulations were carried out assuming a depth-to-diameter ratio (H/D) equal to 2, in accordance with relevant international standards. These standards, together with the assumption of material homogeneity and isotropy, constitute the sole constraints of the present investigation.

The theoretical framework available in the literature is well established, with the exception of the constant value of displacement, which is aligned to the loading direction along the diameter orthogonal to the loading direction. The results obtained in this study enable (1) the determination of this displacement constant, thereby completing the theoretical model; and (2) the characterization of its dependence on the specimen's geometric parameters (diameter D), mechanical properties (Young's modulus E and Poisson's ratio ν), and the applied load intensity P . Specifically, the displacement was found to exhibit a linear relationship with the specimen diameter D , where the slope of this linear trend is a function of both Young's modulus and the applied stress.

Moreover, the outcomes of the numerical analysis led to the formulation of an explicit equation that can be employed for the identification of the mechanical properties of a given material—under the assumption of homogeneity and isotropy—using full-field, contactless measurement techniques such as Digital Image Correlation (DIC) and/or Electronic Speckle Pattern Interferometry (ESPI).

Future work will focus primarily on the analysis of specimens with varying H/D ratios and the experimental validation of the proposed model through an extensive testing campaign.

Author Contributions: Conceptualization, S.B. and L.P.; numerical simulation, A.C.; validation, S.B., A.C. and L.P.; investigation, S.B. and A.C.; writing—original draft preparation, S.B. and A.C.; writing—review and editing, S.B. and L.P.; supervision, L.P. All authors have read and agreed to the published version of the manuscript.

Funding: This research received no external funding.

Institutional Review Board Statement: Not applicable.

Informed Consent Statement: Not applicable.

Data Availability Statement: Data are contained within the article.

Acknowledgments: Authors are grateful to Giuliana Benfratello and Fabio Fontana for their fundamental support during this research.

Conflicts of Interest: The authors declare no conflicts of interest.

References

1. Carneiro, L.L.B. A new method to determine the tensile strength of concrete. In Proceedings of the 5th Meeting of the Brazilian Association for Technical Rules, Rio de Janeiro, Brazil, 16 September 1943; Volume 3, pp. 126–129.
2. Fairbairn, E.M.R. A tribute to Fernando, L.L.B. Carneiro (1913–2001) engineer and scientist who invented the Brazilian test. *Mater. Struct.* **2002**, *35*, 195–196. [[CrossRef](#)]
3. *ASTM D3967-16*; Standard Test Method for Splitting Tensile Strength of Intact Rock Core Specimens. American Society for Testing and Materials: West Conshohocken, PA, USA, 2016.
4. *ASTM C496/C496M*; Standard Test Method for Splitting Tensile Strength of Cylindrical Concrete Specimens. American Society for Testing and Materials: West Conshohocken, PA, USA, 2011.
5. *UNI EN 12390-6:2024*; Testing Hardened Concrete—Part 6: Tensile Splitting Strength of Test Specimens. European Committee for Standardization: Brussels, Belgium, 2024.
6. ISRM. Suggested methods for determining tensile strength of rock materials. *Int. J. Rock. Mech. Min. Sci.* **1978**, *15*, 99–103. [[CrossRef](#)]
7. Yang, L.; Zhang, J.; Shen, J.; Ji, H. Study on the Compressive and Tensile Properties of Latex-Modified Cement Stone. *Materials* **2024**, *17*, 4868. [[CrossRef](#)] [[PubMed](#)]
8. Dong, Q.; Tong, H.; Sun, J.; Peng, S.; Jia, J. Experimental Study of the Dynamic Compressive and Tensile Anisotropic Mechanical Properties and Failure Modes of Shale. *Sensors* **2025**, *25*, 2905. [[CrossRef](#)]
9. Tao, Y.; Wang, J.; Yu, K.; Zhao, J.; Xu, M.; Li, H. Preparing process and the mechanical properties of bi-directionally aligned steel-polypropylene fiber-reinforced cementitious composites. *Case Stud. Constr. Mater.* **2025**, *22*, e04850. [[CrossRef](#)]
10. Timoshenko, S.P.; Goodier, J.N. *Theory of Elasticity*, 3rd ed.; McGraw-Hill: New York, NY, USA, 1988; pp. 233–278.

11. Chen, C.S.; Hsu, S.C. Measurement of Indirect Tensile Strength of Anisotropic Rocks by the Ring Test. *Rock Mech. Rock Eng.* **2001**, *34*, 293–321. [[CrossRef](#)]
12. Chau, K.T.; Wong, R.H.C. Uniaxial compressive strength and point load strength of rocks. *Int. J. Rock. Mech. Min. Sci. Geomech. Abstr.* **1996**, *33*, 183–188. [[CrossRef](#)]
13. Chen, C.h.-S.; Pan, E.; Amadei, B. Determination of deformability and tensile strength of anisotropic rock using Brazilian tests. *Int. J. Rock. Mech. Min. Sci.* **1998**, *35*, 43–61. [[CrossRef](#)]
14. Chen, P.; Xie, H.; Huang, F.; Huang, T.; Ding, Y. Deformation and failure of polymer bonded explosives under diametric compression test. *Pol. Test.* **2006**, *25*, 333–341. [[CrossRef](#)]
15. Choi, Y.; Yuan, R.L. Experimental relationship between splitting tensile strength and compressive strength of GFRC and PFRC. *Cem. Concr. Res.* **2005**, *35*, 1587–1591. [[CrossRef](#)]
16. Claessona, J.; Bohlooli, B. Brazilian test: Stress field and tensile strength of anisotropic rocks using an analytical solution. *Int. J. Rock Mech. Min. Sci.* **2002**, *39*, 991–1004. [[CrossRef](#)]
17. Coviello, A.; Lagioia, R.; Nova, R. On the Measurement of the Tensile Strength of Soft Rocks. *Rock Mech. Rock Eng.* **2005**, *38*, 251–273. [[CrossRef](#)]
18. Guerrero-Miguel, D.J.; Álvarez-Fernández, M.I.; García-Fernández, C.C.; González-Nicieza, C.; Menéndez-Fernández, C. Analytical and numerical stress field solutions in the Brazilian test subjected to radial load distributions and their stress effects at the centre of the disk. *J. Eng. Math.* **2019**, *116*, 29–48. [[CrossRef](#)]
19. Bahaaddini, M.; Serati, M.; Masoumi, H.; Rahimi, E. Numerical assessment of rupture mechanisms in Brazilian test of brittle materials. *Int. J. Solids Struct.* **2019**, *180*, 1–12. [[CrossRef](#)]
20. Jemioło, S. Determining of elastic constants and tensile strength of brittle materials in Brazilian test. In *Concrete and Concrete Structures—Experiments*; Szmigiera, E., Łukowski, P., Jemioło, S., Eds.; Warsaw University of Technology Publishing House: Warszawa, Poland, 2015; pp. 81–92. ISBN 978-83-7814-364-2. (In Polish)
21. Gutierrez-Moizant, R.; Ramirez-Berasategui, M.; Santos-Cuadros, S.; Garcia-Fernandez, C.C. A Novel Analytical Solution for the Brazilian Test with Loading Arcs. *Math. Prob. Eng.* **2020**, *2020*, 2935812. [[CrossRef](#)]
22. Yu, J.; Shang, X. Analysis of the influence of boundary pressure and friction on determining fracture toughness of shale using cracked Brazilian disc test. *Eng. Fract. Mech.* **2019**, *212*, 57–69. [[CrossRef](#)]
23. Kourkoulis, S.K.; Markides, C.F.; Chatzistergos, P.E. The standardized Brazilian disc test as a contact problem. *Int. J. Rock Mech. Min. Sci.* **2013**, *57*, 132–141. [[CrossRef](#)]
24. Serati, M.; Alehossein, H.; Erarslan, N. The Brazilian disc test under a non-uniform contact pressure along its thickness. *Rock Mech. Rock Eng.* **2016**, *49*, 1573–1577. [[CrossRef](#)]
25. Markides, C.F.; Kourkoulis, S.K. Naturally accepted boundary conditions for the Brazilian disc test and the corresponding stress field. *Rock Mech. Rock Eng.* **2013**, *46*, 959–980. [[CrossRef](#)]
26. Japaridze, L. Stress-deformed state of cylindrical specimens during indirect tensile strength testing. *J. Rock Mech. Geotech. Eng.* **2015**, *7*, 509–518. [[CrossRef](#)]
27. Hondros, G. The evaluation of Poisson's ratio and the modulus of materials of a low tensile resistance by the Brazilian (indirect tensile) test with particular reference to concrete. *Aust. J. Basic Appl. Sci.* **1959**, *10*, 243–268.
28. Lu, A.; Wang, S.; Cai, H. Closed-form solution for the stresses in Brazilian disc tests under vertical uniform loads. *Rock Mech. Rock Eng.* **2018**, *51*, 3489–3503. [[CrossRef](#)]
29. Hong, H.; Baranger, T.N. Identification of Bimodular Material Parameters via a Semi—Closed Form Solution of the Brazilian Test. *Exp. Mech.* **2024**, *64*, 805–821. [[CrossRef](#)]
30. Gajewski, M.; Kowalewski, L. Inverse analysis and DIC as tools to determine material parameters in isotropic metal plasticity models with isotropic strain hardening. *Mat. Test.* **2016**, *58*, 818–825. [[CrossRef](#)]
31. Malyszko, L.; Bilko, P.; Kowalska, E. Determination of Elastic Constants in Brazilian Tests Using Digital Image Correlation. In *Proceedings of the 2017 Baltic Geodetic Congress (Geomatics)*, Gdansk, Poland, 22–25 June 2017; Gdansk University of Technology: Gdańsk, Poland, 2017.
32. Benfratello, S.; Cirello, A.; Palizzolo, L.; Sanfilippo, C.; Valenza, A. Experimental Analysis and Numerical Modelling of the Mechanical Behavior of a Sisal-Fiber-Reinforced Geopolymer. *Appl. Sci.* **2024**, *14*, 5216. [[CrossRef](#)]
33. Cirello, A.; Ingrassia, T.; Nigrelli, V. Study of the performances of a fluidynamic actuator. *Int. J. Mech. Eng. Technol.* **2018**, *9*, 859–866.
34. Liu, H.; Jing, H.; Yin, Q.; Zhao, Z.; Meng, Y.; Zhang, L. Study on Mechanical Properties and Fracture Behaviour of Granite after Thermal Treatment under Brazilian Splitting Test. *J. Civ. Eng.* **2023**, *27*, 643–656.
35. Zhou, Y.; Zhang, R.; Zhang, J.; Li, Y.; Li, Z.; Xing, X.; Zhang, Q.; Feng, G. Brazilian splitting testing of the restorative properties of eco-friendly epoxy resin on cracked granite samples with various widths. *Constr. Build. Mater.* **2023**, *401*, 132907. [[CrossRef](#)]
36. Li, X.; Lin, H.; Chen, W.; Liang, S.; Huang, L. A numerical study on the tensile splitting of concrete with digital image processing. *J. Mater. Res. Technol.* **2023**, *25*, 1626–1641. [[CrossRef](#)]

37. Kim, S.Y.; Eum, D.; Lee, H.; Park, K.; Terada, K.; Han, T.S. Evaluating tensile strength of cement paste using multiscale modeling and in-situ splitting tests with micro-CT. *Constr. Build. Mater.* **2024**, *411*, 134642. [[CrossRef](#)]
38. Lei, W.; Wu, Z.; Song, H.; Wang, W.; Cui, H.; Tang, M. 3D Numerical Simulation Study of Brazilian Splitting in Calcite Vein-bearing Shale Based on CT Scans. *KSCE J. Civ. Eng.* **2024**, *28*, 2159–2172. [[CrossRef](#)]
39. Rocco, C.; Guinea, G.V.; Planas, J.; Elices, M. Size effect and boundary conditions in the Brazilian test: Theoretical analysis. *Mater. Struct.* **1999**, *32*, 437–444. [[CrossRef](#)]

Disclaimer/Publisher’s Note: The statements, opinions and data contained in all publications are solely those of the individual author(s) and contributor(s) and not of MDPI and/or the editor(s). MDPI and/or the editor(s) disclaim responsibility for any injury to people or property resulting from any ideas, methods, instructions or products referred to in the content.